

Dependence of the size of copper nanoparticles on laser energy synthesized by pulsed laser ablation in liquid

Prahlad K. Baruah, Ashwini K. Sharma, Alika Khare*

Department of Physics, Indian Institute of Technology Guwahati, Guwahati 781039, India

*Corresponding author, Tel: (+91)36-12582705; E-mail: alika@iitg.ernet.in

Received: 30 March 2016, Revised: 30 September 2016 and Accepted: 15 December 2016

DOI: 10.5185/amp.2017/412

www.vbripress.com/amp

Abstract

In this paper, the effect of incident laser energy on the localized surface plasmon resonance (LSPR) and size of copper (Cu) nanoparticles (NPs) synthesized via pulsed laser ablation of copper in distilled water (DW) is reported. The absorption spectra show plasmon peak in the visible spectral region. The increase in the laser energy from 30 mJ to 70 mJ of the second harmonic of a Q-switched Nd:YAG laser induces a blue shift in the plasmon peak from 627 nm to 617 nm along with its broadening from 180 nm to 242 nm, respectively. These observations have been explained on the basis of the effect of the small size of the NPs formed. The Transmission electron microscope (TEM) substantiates these results as it shows the decrease in the average particle size of the NPs from ~20 nm to ~7 nm with the increase in the incident laser energy from 30 mJ to 70 mJ, respectively. By merely increasing the laser energy, a size-dependent LSPR has been achieved and this can be used as an effective way to control the size of Cu NPs and hence LSPR. Copyright © 2017 VBRI Press.

Keywords: Laser ablation, copper nanoparticles, surface plasmon resonance, nanoparticle size, plasmon bandwidth.

Introduction

Noble metal nanoparticles have received tremendous importance in recent times due to its unique optical and electronic properties [1-3]. Gold, silver and copper exhibits localized surface plasmon resonance (LSPR) due to collective oscillations of free electrons of conduction band in the nanoparticles after interaction with light [4]. The fascination for this property of the metallic nanoparticles dates back to Faraday's time when he observed it and prepared the first stable suspension of gold colloids by reducing gold chloride with phosphorus in water [5]. Gustav Mie, in 1908, was the first to explain this theoretically for spherical particles by solving the Maxwell's equations [6]. Since then, the theory has undergone a number of modifications to explain a lot of other simple systems like spheroid, etc. [7, 8].

Confined electric field associated with SPR excited at the interstitials of nanostructures has already been implemented in large optical field enhancement applications like surface enhanced Raman scattering (SERS), optical sensing, etc. [9, 10]. There have been many reports on surface plasmon based biosensors and its effect [11]. The importance of these versatile sensors are acknowledged by researchers from diverse backgrounds of material science, physics, chemistry, biology and many others which have also resulted in a comprehensive understanding of the phenomena involved [12].

Nanoparticles can be synthesized via chemical reduction, physical vapor condensation, laser ablation, etc. [3, 13]. Pulsed laser ablation of solid in liquid is one of the best and simplest methods for the fabrication of nanoparticles [14, 15]. The process has the advantage of being environment friendly as it does not involve the use of chemicals which have proven to be a major concern for the ecosystem.

Au and Ag have been used extensively for photonic applications but the reactive nature of Cu has limited its use for such applications. However, the low cost and applicability of Cu NPs in various biochemical applications still motivates researchers across the globe to investigate its LSPR properties [16]. LSPR has been experimentally found to be highly dependent on the shape, size and also on the choice of metal used for the synthesis of the nanostructure. The shape and size of the nanostructures of a particular material dictates the spectral signature of its plasmon resonance [17]. Hence, the quest to find ways to control these two parameters in particular and study the effect on the LSPR is indeed a challenging experimental task.

In the present work, copper NPs have been synthesized by pulsed laser ablation in distilled (DW). Keeping in view the importance of controlling the size and shape of the NPs and its dependence on the LSPR, a study of the effect of laser energy delivered onto the copper target on the size of the NPs has been undertaken. An attempt has

also been made to correlate the LSPR (to be mentioned henceforth as SPR only) behaviour and the size of the synthesized NPs. The novelty lies in the fact that by simply increasing the incident laser energy, the size of the Cu NPs and hence SPR can be effectively controlled.

Experimental

Materials

For the synthesis of the Cu NPs, a clean Cu target (99.98% pure, metals basis, SIGMA ALDRICH) was placed at the bottom of a glass beaker filled with 8 mL of DW.

Material synthesis / reactions

The 2nd harmonic of a Q-switched Nd:YAG laser (Model: Litron LPY7864-10G) with a pulse duration of 10 ns was used for ablating the target. The laser was operated at a repetition rate of 10 Hz. The laser beam was steered using a set of optical components and then focused by a 25 cm focal length lens onto the target immersed in DW. To facilitate the availability of fresh area of ablation with each laser shot, the target was continuously moved with the help of a motorized translational stage. To study the effect of laser energy on the properties of Cu NPs, the experiment was performed at laser energies of 30 mJ, 50 mJ and 70 mJ keeping the ablation time fixed for 60 minutes.

Characterizations

The SPR of the synthesized Cu NPs in colloidal form were investigated using a UV-visible spectrophotometer (Model: Shimadzu UV-3101 PC). The NPs were then characterized by the Transmission electron microscope (TEM; Model: JEOL JEM-2100). Particle size and shape were obtained from the TEM images while the selected area electron diffraction (SAED) pattern gave the information about its structural features.

Results and discussion

Copper nanoparticles have been synthesized by varying the laser energy as 30 mJ, 50 mJ and 70 mJ with fixed ablation time of 60 minutes. The change in color of the samples w.r.t the laser energy is clearly visible in Fig. 1.

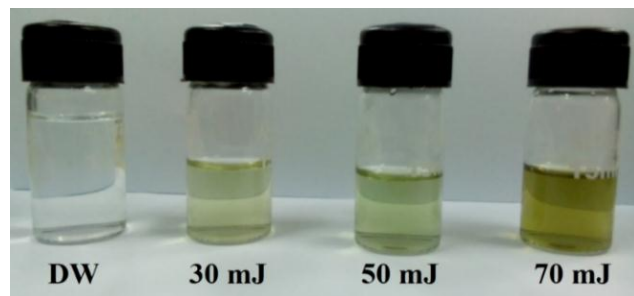


Fig. 1. Change in color of the colloidal solution of Cu NPs.

While the color of the colloidal solution obtained at 30 mJ appears light green, it is darker at 50 mJ and is greenest for the one obtained at 70 mJ. This implies that the concentration of the Cu NPs has increased with the increase in laser energy. This is quite obvious as the laser energy delivered onto the copper target is increased, it facilitates more ablation and hence an enhancement in ejection of particles of target material in the surrounding liquid. This is further confirmed by the absorption spectra of the colloidal solutions as displayed in Fig. 2(a) where an increase in the SPR peak absorbance is clearly seen with the increase in laser energy. The plot of peak absorbance versus laser energy is shown in Fig. 2(b). The SPR peak of Cu usually lies in 570-590 nm range [18]. In the present case, the SPR peak of Cu for all the samples lies in the range of 617-627 nm.

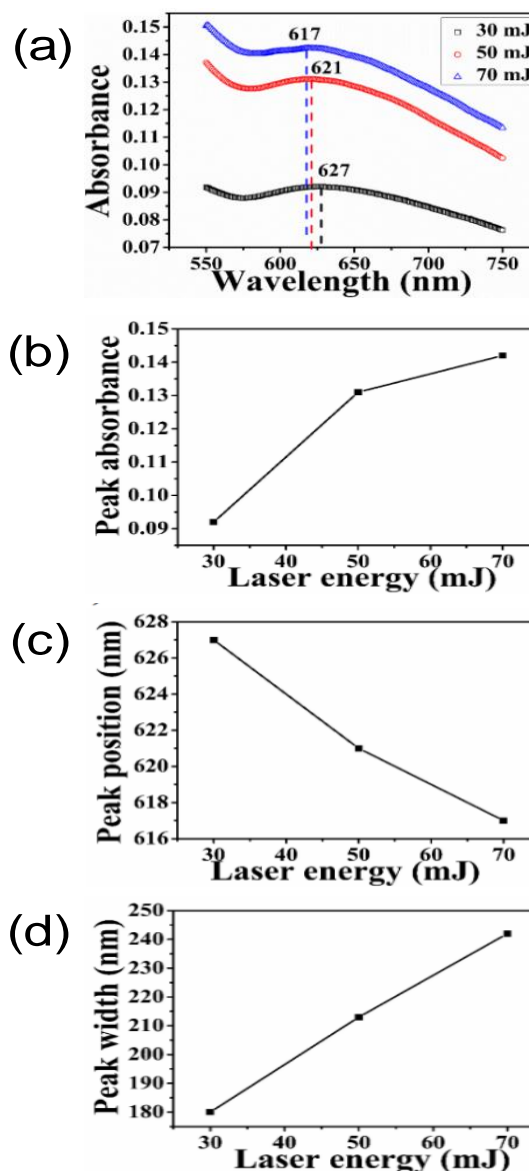


Fig. 2. (a) Absorption spectra of the colloidal solution of Cu NPs synthesized at different laser energies for a laser ablation time of 60 minutes; (b) Variation of SPR peak absorbance with laser energy; (c) Variation of SPR peak position with laser energy; (d) Variation of SPR peak width with laser energy.

This shift in the SPR peak towards longer wavelength can be attributed to the formation of both copper as well as copper oxide NPs, the latter was formed due to oxidation of Cu in DW during ablation [18-19]. The SPR peak position is found to be slightly blue shifted with the increase in laser energy as can be seen in Fig. 2(c). The peak position is at 627 nm for the sample prepared at 30 mJ while it is at 621 nm and 617 nm for 50 mJ and 70 mJ of laser energy, respectively. The SPR band width (FWHM) is found to increase from 180 nm to 242 nm (Fig. 2(d)) with the increase in laser energy. The blue shift of the SPR peak position with the increase in laser energy could be due to the decrease in size of the NPs with the increase in laser pulse energy [20]. This blue shift for small sized particles could be due to quantum confinement effect.

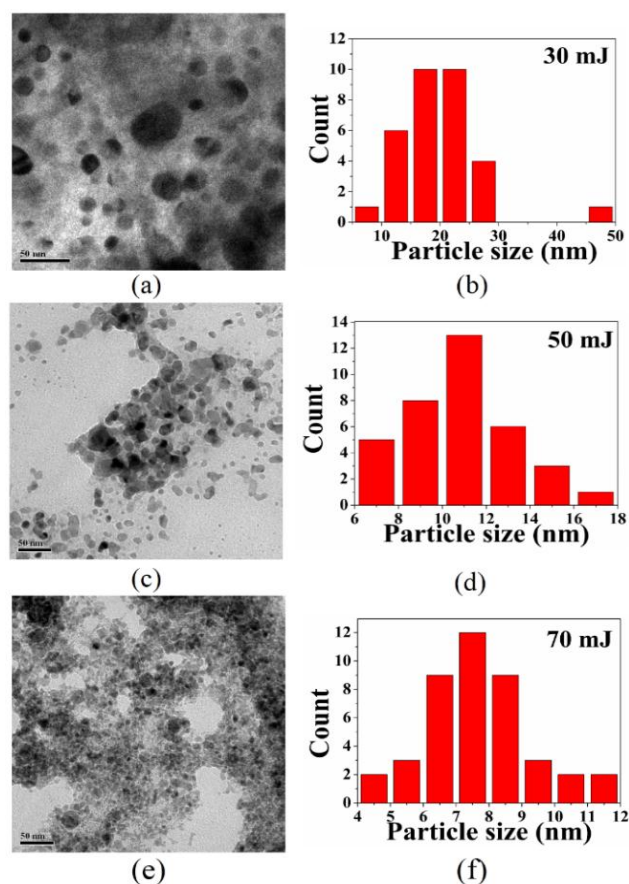


Fig. 3. (a), (c) and (e): TEM image of the synthesized Cu NPs synthesized at 30 mJ, 50 mJ, and 70 mJ, respectively; (b), (d) and (f): Corresponding histograms showing size distribution.

But, for this to hold, the size of the copper/copper oxide NPs should be less than or comparable to its excitonic Bohr radius. From the available literature, this value is reported to be in the range of ~6.67 - 28.7 nm for copper oxide [21]. If the size of the NPs synthesized in the present work lies in this range only then the above speculation of the quantum confinement effect can be said to hold good. As for the increase in bandwidth, this can be explained based on quantum mechanical models provided the size of the synthesized nanoparticles are small [22].

Hence, from the above discussion it is clear that in order to explain both, the behaviour of blue-shift in plasmon peak and its broadening, the determination of the size of the NPs is an absolute necessity. For this, the synthesized NPs are characterized using the TEM. The TEM images of the samples prepared at laser energies of 30 mJ, 50 mJ and 70 mJ for an ablation time of 60 minutes are shown in Fig. 3(a), (c), and (e), respectively and Fig. 3(b), (d), and (f) show the respective histograms of the particle size distribution. The particle size is measured using the Image J software which is available freely. The average particle size of the Cu NPs synthesized at 30 mJ is ~20 nm while for the samples prepared at 50 mJ and 70 mJ it is ~11 nm and ~7 nm, respectively.

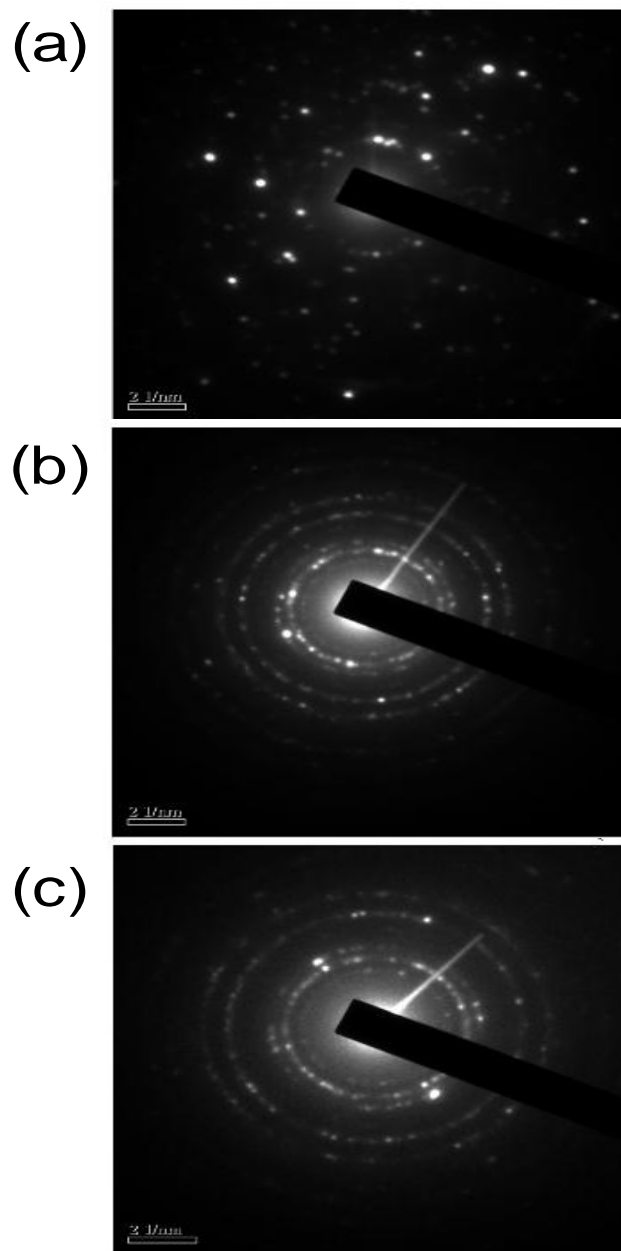


Fig. 4. (a), (b), and (c): SAED pattern of the synthesized Cu NPs synthesized at 30 mJ, 50 mJ and 70 mJ, respectively.

An insight into the structural features of the NPs formed can be obtained from the SAED patterns shown in Fig 4. The NPs synthesized at the laser energy of 30 mJ shows clear crystalline nature whereas those synthesized for higher energies of 50 mJ and 70 mJ shows polycrystalline nature. The interplanar spacings denoted by the d -values are calculated from the SAED patterns. The d -values calculated for the sample prepared at laser energy of 30 mJ are 0.24 nm, 0.20 nm and 0.15 nm corresponding to Cu₂O (111), Cu (111) and CuO (11 $\bar{3}$), respectively. For 50 mJ, the calculated d -values of 0.32 nm, 0.23 nm, 0.20 nm and 0.15 nm correspond to Cu₂O (110), CuO (200), Cu (111) and CuO (11 $\bar{3}$), respectively while for 70 mJ of incident laser energy the d -values of 0.32 nm, 0.23 nm, 0.20 nm correspond to Cu₂O (110), CuO (200) and Cu (111), respectively [18]. Thus, the SAED patterns confirm the formation of both copper as well as copper oxide NPs.

It is seen from the TEM analysis that the determined average particle size in all the three samples lies in the range of the excitonic Bohr radius of copper oxide. Thus, the TEM characterization of the NPs strongly substantiates the fact that the quantum confinement is responsible for the observed blue shift of the plasmon peak [22, 23]. Also, for smaller particles, the $1/r$ dependence (r is the particle diameter) of the plasmon bandwidth has been explained by many theoretical models assuming a size-dependent material dielectric function [22]. The broadening may also be due to the decrease in the mean free path of the electrons [24] which is again viewed as the size confinement of the conduction band electrons in the NPs and is caused by the scattering of the electrons on the NP surface.

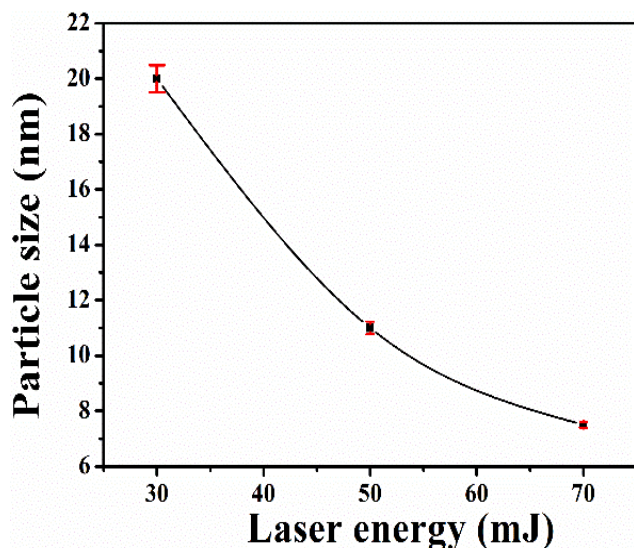


Fig. 5. Plot of the average particle size and laser energy.

A plot of the average particle size and laser energy is shown in Fig. 5 indicating the decrease in the particle size with the increase in laser energy. This may be due to the larger kinetic energy of the ablated species at higher laser energy that increases collision among the initially formed

larger particles in the condensation process leading to fragmentation and hence a decrease in size. Thus, the variation of laser energy can be effectively viewed as a way of tuning the size of NPs and hence its SPR properties.

Conclusion

Cu@Cu_xO ($x=1, 2$) NPs have been synthesized by ablating pure Cu target immersed in DW. The incident laser pulse energy was varied to tune the plasmonic peak behaviour viz. the blue shift and broadening. The size of the NPs has been found to decrease from 20 nm to 7 nm with the increase of laser energy from 30 mJ to 70 mJ, respectively. A correlation between the SPR and size of the NPs synthesized has been established.

Acknowledgements

This work is partially supported by Department of Science and Technology (India), Project No. SR/S2/HEP-18/2009 and I-CUP, Indian Cluster for Ultrafast Photonics supported by the Office of the Principal Scientific Adviser to the Government of India. The authors acknowledge the Central Instruments Facility (CIF), IIT Guwahati, India for the TEM facility.

Author's contributions

Authors have no competing financial interests.

References

- Adams, S.; Zhang, J. Z.; *Coord. Chem. Rev.*, **2016**, 320-321, 18.
DOI: [10.1016/j.ccr.2016.01.014](https://doi.org/10.1016/j.ccr.2016.01.014)
- Jain, P. K.; Huang, X.; El-Sayed, I. H.; El-Sayed, M. A.; *Acc. Chem. Res.*, **2008**, 41, 1578.
DOI: [10.1021/ar7002804](https://doi.org/10.1021/ar7002804)
- Chen, D.; Qiao, X.; Qiu, X.; Chen, J.; *J. Mater. Sci.*, **2009**, 44, 1076.
DOI: [10.1007/s10853-008-3204-y](https://doi.org/10.1007/s10853-008-3204-y)
- Nguyen, T. B.; Thu Vu, T. K.; Nguyen, Q. D.; Nguyen, T. D.; Nguyen, T. A.; Trinh, T. H.; *Adv. Nat. Sci.: Nanosci. Nanotechnol.*, **2012**, 3, 025016.
DOI: [10.1088/2043-6262/3/2/025016](https://doi.org/10.1088/2043-6262/3/2/025016)
- Faraday, M.; *Philos. Trans. R. Soc. London*, **1857**, 147, 145.
- Mie, G.; *Ann. Phys.*, **1908**, 25, 377.
- Acquista, C.; *Appl. Opt.*, **1978**, 17, 3851.
- Rentería-Tapia, V.; Franco, A.; García-Macedo, J.; *J. Nanopart. Res.*, **2012**, 14.
DOI: [10.1007/s11051-012-0915-4](https://doi.org/10.1007/s11051-012-0915-4)
- Israelsen, N. D.; Hanson, C.; Vargis, E.; *Sci. World J.*, **2015**, 124582.
DOI: [10.1155/2015/124582](https://doi.org/10.1155/2015/124582)
- Chen, J. J.; Wu, J. C. S.; Wu, P. C.; Tsai, D. P.; *J. Phys. Chem. C*, **2012**, 116, 26535.
DOI: [10.1021/jp309901y](https://doi.org/10.1021/jp309901y)
- Sepúlveda, B.; Angelomé, P. C.; Lechuga, L. M.; Liz-Marzán, L. M.; *Nano Today*, **2009**, 4, 244.
DOI: [10.1016/j.nantod.2009.04.00](https://doi.org/10.1016/j.nantod.2009.04.00)
- Guo, X.; *J. Biophotonics*, **2012**, 5, 483.
DOI: [10.1002/jbio.201200015](https://doi.org/10.1002/jbio.201200015)
- Ashutosh Tiwari, Atul Tiwari (Eds), In the Nanomaterials in Drug Delivery, Imaging, and Tissue Engineering, John Wiley & Sons, USA, **2013**.
- Yan, Z.; Chrisey, D. B.; *J. Photochem. Photobio., C*, **2012**, 13, 204.
DOI: [10.1016/j.jphotochemrev.2012.04.004](https://doi.org/10.1016/j.jphotochemrev.2012.04.004)
- Yang, G. (Eds.); Laser Ablation in Liquids: Principles and Applications in the Preparation of Nanomaterials; Pan Stanford Publishing: Singapore, **2012**.
- Bogdanović, U.; Lazić, V.; Vodnik, V.; Budimir, M.; Marković, Z.; Dimitrijević, S.; *Mater. Lett.*, **2014**, 128, 75.
DOI: [10.1016/j.matlet.2014.04.106](https://doi.org/10.1016/j.matlet.2014.04.106)

17. Lang, X.; Qian, L.; Guan, P.; Zi, J.; Chen, M.; *Appl. Phys. Lett.*, **2011**, 98, 093701.
DOI: [10.1063/1.3560482](https://doi.org/10.1063/1.3560482)
18. Nath, A.; Khare, A.; *J. Appl. Phys.*, **2011**, 110, 043111.
DOI: [10.1063/1.3626463](https://doi.org/10.1063/1.3626463)
19. Chan, G. H.; Zhao, J.; Hicks, E. M.; Schatz, G. C.; Duyne, R. P. V.; *Nano Lett.*, **2007**, 7, 1947.
DOI: [10.1021/nl070648a](https://doi.org/10.1021/nl070648a)
20. Takami, A.; Kurita, H.; Koda, S.; *J. Phys. Chem. B*, **1999**, 103, 1226.
DOI: [10.1021/jp983503o](https://doi.org/10.1021/jp983503o)
21. Khadivi, H. A.; Vahdati, J. K.; Haddad, M. S.; *J. Ultrafine Grained Nanostruct. Mater.*, **2015**, 48, 37.
DOI: [10.7508/jufgmsm.2015.01.006](https://doi.org/10.7508/jufgmsm.2015.01.006)
22. Link, S.; El-Sayed, M. A.; *J. Phys. Chem. B*, **1999**, 103, 8410.
DOI: [10.1021/jp9917648](https://doi.org/10.1021/jp9917648)
23. Haider, A. F. M. Y.; Sengupta, S.; Abedin, K. M.; Talukder, A. I.; *Appl. Phys. A: Mater. Sci. Process*, **2011**, 105, 487.
DOI: [10.1007/s00339-011-6542-6](https://doi.org/10.1007/s00339-011-6542-6)
24. Mogensen, K. B.; Kneipp, K.; *J. Phys. Chem. C*, **2014**, 118, 28075.
DOI: [10.1021/jp505632n](https://doi.org/10.1021/jp505632n)